

An auto weather-vaning system for a DP vessel that uses a nonlinear controller and a disturbance observer

Dae Hyuk Kim and Nakwan Kim

Department of Naval Architecture and Ocean Engineering, Seoul National University, Korea

ABSTRACT: *An auto weather-vaning system for a Dynamic Positioning (DP) vessel is proposed. When a DP vessel is operating, its position keeping is hindered by ocean environmental disturbances which include the ocean current, wave and wind. Generally, most ocean vessels have a longitudinal length that is larger than the transverse width. The largest load acts on the DP vessel by ocean disturbances, when the disturbances are incoming in the transverse direction. Weather-vaning is the concept of making the heading angle of the DP vessel head toward (or sway from) the disturbance direction. This enables the DP vessel to not only perform marine operations stably and safely, but also to maintain its position with minimum control forces (surge & sway components). To implement auto weather-vaning, a nonlinear controller and a disturbance observer are used. The disturbance observer transforms a real plant to the nominal model without disturbance to enhance the control performance. And the nonlinear controller deals with the kinematic nonlinearity. The auto weather-vaning system is completed by adding a weather-vaning algorithm to disturbance based controller. Numerical simulations of a semi-submersible type vessel were performed for the validation. The results show that the proposed method enables a DP vessel to maintain its position with minimum control force.*

KEY WORDS: Dynamic positioning (DP); Weather-vaning; Nonlinear controller; Disturbance observer.

INTRODUCTION

Dynamic Positioning (DP) is an automatic position control system using propellers or thrusters for offshore floating structures. Recently, the maritime operation area has expanded into the deep sea. Because a mooring system is not economically feasible in the deep sea, DP has been studied more than ever before, by many research groups. In particular, ocean prospectors, like drilling rigs or drill ships, have to move around in an oilfield development zone, so a DP capability analysis is performed in the basic design stage of these vessels.

The position and velocity vectors of a DP vessel are measured by the Differential Global Positioning system (DGPS) / Inertial Navigation System (INS) in real time. The measured position and velocity vectors contain measurement noise and process noise. The main process noise can be regarded as environmental disturbances that threaten the survivability of a structure, and interfere with its stable operation. Thus, disturbances are an important matter, which must be taken into consideration. But the most common DP control system has a simple linear controller, combined with a wind feedforward controller, in which there is no consideration of other disturbances (ocean current or wave load). Moreover, because the wind feedforward controller is designed based on experimental data or empirical regression formula, it may not be possible to compensate for the wind load

Corresponding author: *Nakwan Kim*, e-mail: nwkim@snu.ac.kr

This is an Open-Access article distributed under the terms of the Creative Commons Attribution Non-Commercial License (<http://creativecommons.org/licenses/by-nc/3.0>) which permits unrestricted non-commercial use, distribution, and reproduction in any medium, provided the original work is properly cited.

exactly. It is hard to estimate and to compensate for ocean environmental disturbances in real time, so the control system has to be designed with consideration of not just the dynamical characteristics of an ocean structure, but also unknown ocean disturbances.

Weather-vaning is to make the heading angle of a DP vessel head towards (or away from) for the disturbance direction. Most ocean floating structures have long longitudinal length. So the disturbance incoming in the transverse direction of a DP vessel induces larger force and moment, compared with the longitudinal direction. Weather-vaning enables a DP vessel to maintain its position with minimum control force through matching the heading angle of a DP vessel with the disturbance direction.

In this paper, an auto weather-vaning system for a DP vessel using a nonlinear controller and disturbance observer is proposed. It is almost impossible to measure the exact force and moment induced by ocean environmental disturbances (the ocean current, wave and wind) in real time. It can be called the disturbance uncertainty, which degrades the performance of a designed controller. Generally, a controller is designed by using only a plant model without disturbance, so the control performance of the closed-loop system does not have to be as good as expected. To deal with this problem, the disturbance observer is introduced. It guarantees the robustness of the closed-loop system, by transforming a real plant, into a nominal model without disturbance. The weather-vaning system continuously changes the heading angle of a DP vessel. Because of kinematic non-linearity, a nonlinear control method is more efficient than a linear control method. This paper used a backstepping controller as the DP controller, which has already been proven for its stability and performance by several research groups.

Since the late 1990s, there have been many studies of DP controllers and observers. A mathematical model of a DP vessel was constructed, and an LQG feedback controller and a model reference feedforward controller were proposed by [Sørensen \(1996\)](#). A nonlinear controller for ocean structures, like a feedback linearization and backstepping, was presented ([Fossen, 1994; 2002](#)). [Sørensen \(2011\)](#) wrote a survey paper that contains a lot of previous research materials about DP controllers and observers. The research about a disturbance observer has been studied by electrical and mechanical field research groups ([Radke and Gao, 2006; Schrijver and Dijk, 2002; Shim and Joo, 2007; Choi et al., 2003](#)). The research about a nonlinear observer to estimate the angle of attack for a missile autopilot system in the presence of the model uncertainties ([Lee et al., 2011](#)). But the researches in which a disturbance observer is applied to the DP system have not been studied. Ocean structures are always unavoidably exposed to disturbances, so it is most appropriate to apply a disturbance observer to ocean structures. There are a few researches about weather-vaning systems. Most papers about weather-vaning have focused on passive weather-vaning, which only depends on the yaw moment induced by disturbances, without any active actuator operations ([Chilliamcharla et al., 2009; Morandini and Wong, 2007](#)). The paper performs the motion analysis of a DP vessel that is free to rotate in the yaw direction. [Fossen and Strand \(2001\)](#) proposed Weather Optimal Positioning Control (WOPC) for a DP vessel. The methodology in that paper enables a DP vessel to minimize energy consumption, by introducing a gravity field concept into 3 DOF horizontal planes. It can be said that this is a kind of active weather-vaning system, by using actuators. But in this methodology, there is no consideration of the magnitude and frequency characteristics of disturbances. On the other hand, a disturbance observer for a weather-vaning system can be designed based on the consideration of the disturbance characteristics.

The paper is described in the following order. First of all, the mathematical model of a DP vessel is described. The mathematical model is composed of two parts. One is the low-frequency model, and the other is the wave-frequency model. In the model, the characteristics of disturbances are described. The ocean current, wind and wave are described respectively. Then, the controller and the disturbance observer are described. The basic concepts are briefly explained, and the design procedures are explained in detail. Next, a weather-vaning algorithm is explained. The effectiveness of the proposed method is validated, by the numerical simulations of a semi-submersible type vessel. Finally, the conclusion summarizes the research results.

MATHEMATICAL MODEL

First of all, the coordinate systems for a mathematical model are defined. The dynamic model for a DP vessel consists of two parts ([Sørensen, 1996; Fossen, 2002](#)). One is a linear wave-frequency model, and the other is a nonlinear low-frequency model. The linear wave-frequency model is about an oscillatory motion induced by a linear wave. It is zero-mean oscillatory motion that has high frequency, so it not only has bad influence on actuators, and but also belongs to uncontrollable motion. The nonlinear low-frequency model is of the slowly varying motion induced by environmental disturbances, which accounts for

the ocean current, and second order wave and wind loads. This motion has low frequency, and makes a DP vessel move away from its desired position. Thus it is the motion that must be controlled for stable operation. But because the DGPS/INS measures these two motions together, the wave frequency motion is generally filtered by a low pass filter or observer system.

Kinematics

Two different reference frames are defined. There are the earth-fixed reference frame $O - XYZ$, and the body-fixed reference frame $O_b - x_b y_b z_b$. These are illustrated in Fig. 1.

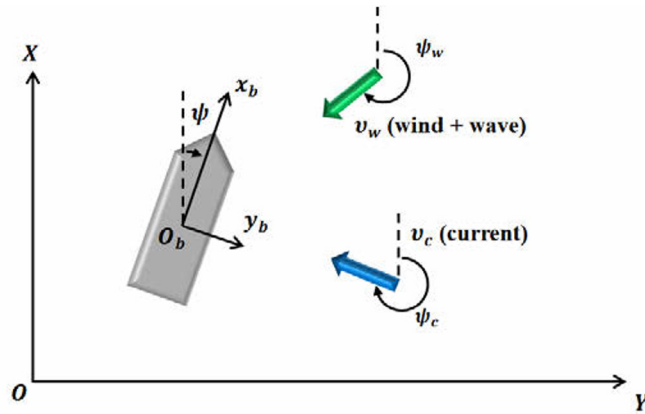


Fig. 1 Reference frames for a DP vessel.

If only 3 DOF horizontal motions (surge, sway and yaw) are considered, the earth-fixed position vector and the body-fixed velocity vector are given by reference frames for a DP vessel:

$$\eta = [x \quad y \quad \psi]^T, \quad v = [u \quad v \quad r]^T \tag{1}$$

The 3 DOF relation between the body-fixed frame and the earth-fixed frame is as follows:

$$\dot{\eta} = R(\psi)v \tag{2}$$

where, $R(\psi) = \begin{bmatrix} \cos \psi & -\sin \psi & 0 \\ \sin \psi & \cos \psi & 0 \\ 0 & 0 & 1 \end{bmatrix}$

Linear wave-frequency model

The linear wave-frequency model is considered as the motion induced by irregular wave, which is the linear superposition of first order waves with different frequencies and amplitudes. It can be said that the analysis of this motion is the same as the conventional seakeeping problem (Lewis, 1989). The 6 DOF equations of motion are formulated as:

$$(-\omega^2 [M_{RB} + A(\omega)] - j\omega B(\omega) + C)\xi(j\omega) = \tau_{1st_wave}(j\omega) \tag{3}$$

where, $\xi(j\omega) \in R^6$ is the 6 DOF position vector, and $\tau_{wave_1st}(j\omega) \in R^6$ is the first order wave excitation vector. $M_{RB} \in R^{6 \times 6}$ is the system inertia matrix, and $C \in R^{6 \times 6}$ is the linearized restoring matrix. $A(\omega) \in R^{6 \times 6}$ and $B(\omega) \in R^{6 \times 6}$ are the added mass and damping coefficient matrix which are a function of wave frequency, so the above equation (3) is repre-

sented in the frequency domain. The motion spectrum by the first order wave excitation is calculated by using the wave spectrum and Response Amplitude Operator (RAO) of a vessel. Even though this motion cannot be controlled, because the motion is a relatively high frequency motion, it should be considered. The reason is that the position or velocity vectors measured by the measurement equipment of a DP vessel include this motion. Generally, a low-pass filter is used to filter out the motion.

Nonlinear low-frequency model

The nonlinear low-frequency model is considered as the motion induced by environmental disturbances which consist of the ocean current, second order wave and wind loads. The first order wave does not induce the drift motion, so it is not included in environmental disturbances. The analysis of this motion is similar to the conventional ship maneuvering problem (Lewis, 1989). But the model has several environmental disturbances, unlike the maneuvering problem. It is assumed that the disturbances induce only 3 DOF horizontal motions.

$$M\dot{v} + C_{RB}(v)v + C_A(v_r)v_r + D(v_r)v_r = \tau_{con} + d \tag{4}$$

where, $v \in R^3$ is the 3 DOF horizontal velocity vector, and $v_r \in R^3$ is the 3 DOF horizontal relative velocity vector between a vessel and the ocean current. $\tau_{con} \in R^3$ is the control force and moment vector by actuators, and $d \in R^3$ is the force and moment vector by environmental disturbances. $M \in R^{3 \times 3}$ is the system inertia matrix, including the added mass and added mass moment of inertia. $C_{RB}(v) \in R^{3 \times 3}$ and $C_A(v) \in R^{3 \times 3}$ are the Coriolis and centripetal matrices of the vessel and the added mass and added mass moment of inertia. $D(v_r) \in R^3$ is the linear and nonlinear damping matrix. In the consideration of the general characteristics of ships or ocean structures, the following assumptions can be used:

- i) The body-fixed frame is located at the principal axis frame.

$$I_{xy} = I_{yz} = I_{xz} = 0$$

- ii) The mass of the DP Vessel is distributed symmetrically to the left and right.

$$y_g = 0$$

- iii) All hydrodynamic coefficients are constant.

In (4), all of the matrices can be written:

$$M = \begin{bmatrix} m - X_{\dot{u}} & 0 & 0 \\ 0 & m - Y_{\dot{v}} & mx_g - Y_{\dot{r}} \\ 0 & mx_g - N_{\dot{v}} & I_{zz} - N_{\dot{r}} \end{bmatrix}, \quad C_{RB}(v) = \begin{bmatrix} 0 & 0 & -m(x_g r + v) \\ 0 & 0 & mu \\ m(x_g r + v) & -mu & 0 \end{bmatrix}$$

$$D(v)v = Dv + D_n(v)v, \quad D = -\begin{bmatrix} X_u & 0 & 0 \\ 0 & Y_v & Y_r \\ 0 & N_v & N_r \end{bmatrix}, \quad D_n(v)v = \begin{bmatrix} 0.5\rho C_X A_X u |u| \\ 0.5\rho (A_y / L_{pp}) C_{Y,2D} \int_{-0.5L_{pp}}^{0.5L_{pp}} (v + xr) |v + xr| dx \\ 0.5\rho (A_y / L_{pp}) C_{Y,2D} \int_{-0.5L_{pp}}^{0.5L_{pp}} x (v + xr) |v + xr| dx \end{bmatrix}$$

$$\tau_{con} = [\tau_x \quad \tau_y \quad \tau_{\psi}]^T, \quad d = [X_{2nd_wave} + X_{wind} \quad Y_{2nd_wave} + Y_{wind} \quad N_{2nd_wave} + N_{wind}]^T$$

The nonlinear part in the damping matrix $D_n(v)$ is calculated by the surge viscous resistance, and the cross-flow drag principle (Faltinsen, 1990). In the cross-flow drag, one 2D drag coefficient computed by using Hoerner's approximation is used, instead of 2D drag coefficients for each section. By eliminating the integrals, the nonlinear damping part is expressed in second order modulus form:

$$D_n(v) = - \begin{bmatrix} X_{|u|u} |u| & 0 & 0 \\ 0 & Y_{|v|v} |v| + Y_{|r|r} |r| & Y_{|v|r} |v| + Y_{|r|v} |r| \\ 0 & N_{|v|v} |v| + N_{|r|r} |r| & N_{|v|r} |v| + Y_{|r|r} |r| \end{bmatrix} \quad (5)$$

Ocean environmental disturbances

As previously mentioned, ocean environmental disturbances include the ocean current, and second order wave and wind loads. The force and moment by the ocean current are considered as the relative velocity between a vessel and the current velocity. The nonlinear low-frequency model is described in the body-fixed frame, so the earth-fixed current velocity vector has to be transformed to the body-fixed current velocity vector. The relationship between the two vectors is as follow:

$$\begin{aligned} v_c &= \begin{bmatrix} \cos \psi & \sin \psi \\ -\sin \psi & \cos \psi \end{bmatrix} \begin{bmatrix} U_c \cos \psi_c \\ U_c \sin \psi_c \end{bmatrix} \\ &= U_c \begin{bmatrix} \cos \psi \cos \psi_c + \sin \psi \sin \psi_c \\ -\sin \psi \cos \psi_c + \cos \psi \sin \psi_c \end{bmatrix} \\ &= U_c \begin{bmatrix} \cos(\psi_c - \psi) \\ \sin(\psi_c - \psi) \end{bmatrix} \end{aligned} \quad (6)$$

where, v_c is the ocean current velocity vector in the body-fixed frame. U_c is the speed of the ocean current, ψ and ψ_c are the yaw angle of a vessel and the direction of the ocean current respectively. The relative velocity vector between a vessel and the ocean current is defined as follow:

$$v_r = v - v_c \quad (7)$$

The relative velocity is used in the nonlinear low-frequency model (4).

The second order wave loads is divided into mean, slowly varying loads and rapidly varying motion. It can be calculated by means of quadratic transfer functions for, $i=1..6$ (Newman, 1997; Faltinsen, 1990). The effect of the rapidly varying wave loads can be neglected, because it has high frequencies.

$$w_{2nd_wave}^i = \sum_{j=1}^N \sum_{k=1}^N A_j A_k \left[T_{jk}^{ic} \cos((\omega_k - \omega_j)t + \varepsilon_k - \varepsilon_j) + T_{jk}^{is} \sin((\omega_k - \omega_j)t + \varepsilon_k - \varepsilon_j) \right] \quad (8)$$

where, A_j , ω_j and ε_j are a j -component wave amplitude, wave frequency and random phase respectively. T_{jk} is the quadratic transfer functions which is obtained by using the wave velocity potential. In the consideration of the mean wave load which is the case of $k=j$, T_{kk} can be calculated by the first order wave velocity potential. Generally, T_{jk} does not vary with the frequencies, then the following approximations are satisfied (Newman, 1977).

$$\begin{aligned} T_{jk}^{ic} &= T_{kj}^{ic} = \frac{1}{2} (T_{jj}^{ic} + T_{kk}^{ic}) \\ T_{jk}^{is} &= T_{kj}^{is} = 0 \end{aligned} \quad (9)$$

By the approximations, the slowly-varying load is included in the mean drift load. Eventually, the wave drift load can be defined by dividing the wave spectrum into N equal frequency intervals with frequency ω_j , amplitude A_j and phase ε_j (Sørensen, 2011).

$$\tau_{2nd_wave}^i = 2 \left(\sum_{j=1}^N A_j \left(T_{jj}^i(\omega_j, \beta_{wave} - \psi) \right)^{1/2} \cos(\omega_j t + \varepsilon_j) \right)^2 \quad (10)$$

where $T_{jj}^i > 0$ is the frequency-dependent wave drift function, and β_{wave} is the mean wave direction. 3 DOF horizontal second order wave force and moment can be expressed as follows:

$$\begin{aligned} X_{2nd_wave} &= W_{2nd_wave}^1 \\ Y_{2nd_wave} &= W_{2nd_wave}^2 \\ N_{2nd_wave} &= W_{2nd_wave}^6 \end{aligned} \quad (11)$$

There are several regression methods to estimate the force and moment by the wind for marine structures (Blendermann, 1995; Gould, 1982; Isherwood, 1972; OCIMF, 1994). But these methods have been developed for ships. There is a research about the wind load for pontoon type floating structures (Kitamura et al., 1997). All of the estimated methods need the specific geometric information of the upper structures of a vessel. It is hard to know this exact information, so it is difficult to implement the wind load. This study assumes the wind load of a DP vessel is similar to that of other vessels with similar size. The regression parameters of Isherwood (1972) are used.

$$\begin{aligned} X_{wind} &= \frac{1}{2} C_X (\gamma_{wind}) \rho_a V_r^2 A_T \\ Y_{wind} &= \frac{1}{2} C_Y (\gamma_{wind}) \rho_a V_r^2 A_L \\ N_{wind} &= \frac{1}{2} C_N (\gamma_{wind}) \rho_a V_r^2 A_L L \end{aligned} \quad (12)$$

where, C_X , C_Y and C_N are empirical coefficients determined by the geometric characteristics of a vessel, γ_{wind} is the relative angle of the wind and a vessel, ρ_a is the density of air, V_{wind} is the wind speed, A_T and A_L are the transverse and lateral projected areas, and L is the length of a vessel.

CONTROLLER DESIGN

This paper proposes a nonlinear controller to control the 3 DOF horizontal (surge, sway and yaw) position vector. The nonlinear control method has the advantage of exactly dealing with a nonlinear system, but it also has the disadvantage of the difficulty of designing a controller, and analyzing its stability. On the other hand, the linear control method has been well developed by many previous studies, so that most industries have mainly used the linear control method. The DP is also no exception. Most of the DP control systems use a linear controller. However, because our eventual goal is the weather-vaning, the designed controller is capable of not only maintaining the desired position, but also changing the yaw angle of a vessel at the same time. Because of the nonlinearity of a DP vessel's kinematics, the exact position vector cannot be expressed as a linearized rotation matrix. For this reason, a nonlinear control method is used as the DP controller, instead of a linear control method. From the 1990s, some nonlinear control methods for a DP control system have been researched. They are well documented in some books and papers (Sørensen, 2011; Fossen, 2002). Among nonlinear control methods, the backstepping control method is used in this paper. The backstepping control method was developed for nonlinear dynamical systems in the early 1990s (Kokotovic, 1992; Lozano and Brogliato, 1992). This method determines a control law through the recursive

construction of a Lyapunov function candidate step-by-step. A stabilizing function and a backstepping variable are defined in each design step and the actual control input is determined in the last design step. Because each design step is affected by the immediately previous design step, the design procedure of the controller is simple. In other words, the construction of Lyapunov function candidates and the control gain selection are easy. The stability of the nonlinear closed loop system is easily verified theoretically, by using the Lyapunov stability theorem. The design process of the backstepping controller for a DP vessel is explained in reference Fossen (2002). First of all, the design goal is to make the position vector $\eta = [x \ y \ \psi]^T$ defined in (2) follow the desired position vector $\eta_d = [x_d \ y_d \ \psi_d]^T$. Only the kinematics model (2) and the low-frequency model (4) are considered.

Design step 1

The first backstepping variable z_1 is defined as an error value between the 3 DOF horizontal position vector and the desired position vector.

$$z_1 = \eta - \eta_d \quad (13)$$

The time differentiation of (13) is as follows:

$$\begin{aligned} \dot{z}_1 &= \dot{\eta} - \dot{\eta}_d \\ &= R(\psi)[v - v_d] \end{aligned} \quad (14)$$

The velocity vector v is set to a virtual control, which makes the first backstepping variable be zero.

$$v = \alpha_1 + z_2 \quad (15)$$

α_1 is the stabilizing function to make the z_1 -system (14) stable. z_2 is the second backstepping variable, which is defined as an error value between the virtual control v , and the stabilizing function α_1 .

$$\dot{z}_1 = R(\psi)[\alpha_1 + z_2 - v_d] \quad (16)$$

A first Lyapunov function candidate for the z_1 -system is defined.

$$V_1 = \frac{1}{2} z_1^T z_1 \quad (17)$$

The time differentiation of (17) is as follows:

$$\begin{aligned} \dot{V}_1 &= z_1^T \dot{z}_1 \\ &= z_1^T R(\psi)[\alpha_1 + z_2 - v_d] \end{aligned} \quad (18)$$

To make (18) negative about z_1 , the stabilizing function α_1 is chosen, as follows:

$$\alpha_1 = -R^T(\psi)K_1 z_1 + v_d \quad (19)$$

$R(\psi)$ is an orthogonal matrix, so $R(\psi)R^T(\psi) = I$ is satisfied. K_1 is a control gain matrix. Diagonal elements in the

matrix are control gains for the surge, sway and yaw motion, respectively. To control each motion independently, all off-diagonal terms are zero.

$$K_1 = \begin{bmatrix} k_{1x} & 0 & 0 \\ 0 & k_{1y} & 0 \\ 0 & 0 & k_{1\psi} \end{bmatrix} \quad (20)$$

By substituting (19) into (16) and (18), we can get

$$\dot{z}_1 = -K_1 z_1 + R(\psi) z_2 \quad (21)$$

$$\begin{aligned} \dot{V}_1 &= z_1^T [-K_1 z_1 + R(\psi) z_2] \\ &= -z_1^T K_1 z_1 + z_1^T R(\psi) z_2 \end{aligned} \quad (22)$$

The above (22) cannot be negative, because of the second term $z_1^T R(\psi) z_2$. It will be eliminated in the next design step.

Design step 2

The second backstepping variable z_2 has already been defined in (15). The time differentiation of z_2 is as follows:

$$\dot{z}_2 = \dot{v} - \dot{\alpha}_1 \quad (23)$$

To use the dynamical model of 3 DOF horizontal motions (4), multiply (23) by the inertia matrix M .

$$\begin{aligned} M\dot{z}_2 &= M\dot{v} - M\dot{\alpha}_1 \\ &= \tau + w - C_{RB}(v)v - C_A(v_r)v_r - D(v_r) - M\dot{\alpha}_1 \end{aligned} \quad (24)$$

Because the mathematical model of a DP vessel is a second order differential system, any virtual control or backstepping variables are no longer needed, and the actual control input τ appears in this second design step. A second Lyapunov function candidate is defined as follows:

$$V_2 = V_1 + \frac{1}{2} z_2^T M z_2 \quad (25)$$

By substituting (24) into the time differentiation of (25), we can get:

$$\begin{aligned} \dot{V}_2 &= \dot{V}_1 + z_2^T M \dot{z}_2 \\ &= -z_1^T K_1 z_1 + z_1^T R(\psi) z_2 + z_2^T [\tau + d - C_{RB}(v)v - C_A(v_r)v_r - D(v_r) - M\dot{\alpha}_1] \end{aligned} \quad (26)$$

To make (26) negative, the actual control input τ is chosen as:

$$\tau = -\hat{d} + C_{RB}(v)v + C_A(v_r)v_r + D(v_r) + M\dot{\alpha}_1 - K_2 z_2 - R^T(\psi) z_1 \quad (27)$$

where \hat{d} is the estimated value of the disturbance by the disturbance observer. K_2 is another control gain matrix:

$$K_2 = \begin{bmatrix} k_{2x} & 0 & 0 \\ 0 & k_{2y} & 0 \\ 0 & 0 & k_{2w} \end{bmatrix} \tag{28}$$

By substituting (27) into (23) and (26), we can get:

$$M\dot{z}_2 = -R^T(\psi)z_1 - K_2z_2 - \hat{d} + d \tag{29}$$

$$\dot{V}_2 = -z_1^T K_1 z_1 - z_2^T K_2 z_2 + z_2^T (d - \hat{d}) \tag{30}$$

If the disturbance observer eliminates the disturbance exactly, the time differentiation of the second Lyapunov function candidate can be strictly negative about the backstepping variables z_1 and z_2 .

$$\dot{V}_2 = -z_1^T K_1 z_1 - z_2^T K_2 z_2 < 0 \tag{31}$$

By the Lyapunov Stability theorem, $z_1 \rightarrow 0$ and $z_2 \rightarrow 0$ as $t \rightarrow \infty$, then $\eta \rightarrow \eta_d$ as $t \rightarrow \infty$. This means the position vector follows the desired position vector, as time goes by.

DISTURBANCE OBSERVER

The basic concept of the disturbance observer is to use an inverse nominal model to eliminate the disturbance and modeling uncertainty. It is easy to combine a closed loop system with the disturbance observer, because it constitutes an inner-loop. The basic structure of the disturbance observer is illustrated in Fig. 2.

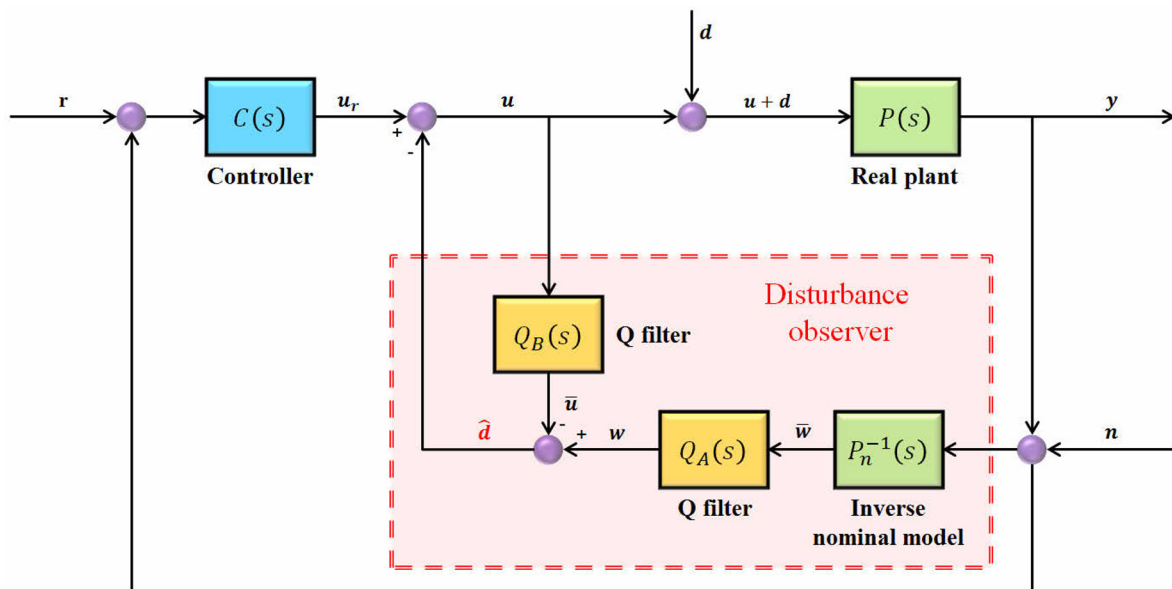


Fig. 2 The structure of the disturbance observer.

In Fig. 3, $P(s)$ is a real plant, $P_n(s)$ is the nominal model of the real plant, and $C(s)$ is the controller. $Q_A(s)$ and $Q_B(s)$ are the same Q – filter, of which the relative degree is larger than the degree of the nominal model, to enable the implementation. r is the reference input, u is the control input, d is the disturbance, n is noise, \bar{w} is the estimated value

of $u+d$, and \hat{d} is the estimated value of the disturbance. To briefly explain how the disturbance observer works, frequency domain analysis about the disturbance observer is described (Shim et al., 2009). The output of the real plant is expressed as follows:

$$y(s) = T_{yr}(s)r(s) + T_{yd}(s)d(s) - T_{yn}(s)n(s) \tag{32}$$

$$T_{yr}(s) = \frac{PP_nC}{P_n(1+PC)+Q(P-P_n)}, \quad T_{yd}(s) = \frac{PP_n(1-Q)}{P_n(1+PC)+Q(P-P_n)}, \quad T_{yn}(s) = \frac{P(Q+P_nC)}{P_n(1+PC)+Q(P-P_n)}$$

If $Q(s) \approx 1$, the transfer functions of (32) are approximated as follows:

$$y(s) = T_{yr}(s)r(s) - T_{yn}(s)n(s) \tag{33}$$

$$T_{yr}(s) \approx \frac{P_nC}{1+P_nC}, \quad T_{yd}(s) \approx 0, \quad T_{yn}(s) \approx 1$$

Generally, the disturbance is a low-frequency component, and noise is a high-frequency component. In the low-frequency region, the output is considered as follows:

$$y(s) \approx \frac{P_nC}{1+P_nC}r(s) \tag{34}$$

$Q(s)$ is designed as a low-pass filter with DC gain 1, to implement $Q(s) \approx 1$. This shows the disturbance observer changes the closed-loop system into the nominal model without the disturbance, under the assumption that all transfer functions are stable, and $Q(s)$ is a low-pass filter with sufficiently large bandwidth (Khalil, 2002). Thus, the outer-loop controller $C(s)$ can be designed, without the consideration of the disturbance and modeling uncertainty. $Q(s)$ is generally designed as follows:

$$Q(s) = \frac{c_k(\tau s)^k + c_{k-1}(\tau s)^{k-1} + \dots + c_0}{(\tau s)^l + a_{l-1}(\tau s)^{l-1} + \dots + a_1(\tau s) + a_0} \tag{35}$$

where, $l \geq k + \deg(P_n)$ and $a_0 = c_0$. The coefficients a_i of $Q(s)$ are chosen such that $a^l + a_{l-1}s^{l-1} + \dots + a_1s + a_0$ is a Hurwitz polynomial. The parameter τ determines the cut-off frequency.

To design the disturbance observer for a DP vessel, the nominal model of a real plant is determined, and the relative degree of the nominal model is examined. First of all, the low-frequency motion (4) is linearized at the point that all states are zero.

$$M\dot{v}_r + Dv_r = \tau_{con} + d \tag{36}$$

The state space form of (4) is as follows:

$$\dot{v}_r = -M^{-1}Dv_r + M^{-1}(\tau_{con} + d) \tag{37}$$

The determinant of the system inertia matrix M has to be checked as to whether it is invertible or not.

$$\det(M) = (m - X_{\ddot{u}}) \left[(m - Y_{\dot{v}})(I_{zz} - N_{\dot{r}}) - (mx_g - Y_{\dot{r}})(mx_g - N_{\dot{v}}) \right] \tag{38}$$

Because $X_{\ddot{u}}$ is the surge added mass, it has negative sign, so $(m - X_{\ddot{u}})$ is of positive value. In general ships and offshore structures, the hydrodynamic pressure center and the gravity center are very closer to the center of the body-fixed coordinate, so $Y_{\dot{r}}$, $N_{\dot{v}}$ and x_g are of small value. Thus, the relationship $(m - Y_{\dot{v}})(I_{zz} - N_{\dot{r}}) \gg (mx_g - Y_{\dot{r}})(mx_g - N_{\dot{v}})$ is always satisfied, and $\det(M) \neq 0$. (37) can be represented by a state space form, as follows:

$$\dot{x} = Ax + B(\tau_{con} + d) \tag{39}$$

where, $x = v_r \in R^{3 \times 1}$, $A = -M^{-1}D \in R^{3 \times 3}$, $B = M^{-1} \in R^{3 \times 3}$

In order to estimate the disturbance d , the above equation (39) is transformed in the s -domain. It is assumed to be full state feedback. The inverse nominal model is an improper transfer matrix. For implementation, a Q -filter $Q(s)$ is introduced.

$$\hat{d} = Q(s) \left[B^{-1}(sI - A)X(s) - \tau_{con} \right] \tag{40}$$

In (40), the estimated disturbance \hat{d} involves the ocean current, wind and wave loads. It is assumed that the 3 DOF horizontal control force and moment τ_{con} control 3 DOF horizontal motions (surge, sway and yaw) independently. Each of the disturbance observers for 3 DOF horizontal motions can be applied, respectively. It can be easily known that the relative degree of the nominal model of a DP vessel is less than 2, regardless of the values in the matrices A and B . Thus $Q(s)$ is designed as a low-pass filter with the relative degree 2. A high order low-pass filter can be designed by using a Butterworth filter. The cut-off frequency of the filter is determined by a consideration of the frequency characteristics of the disturbance. Because the control target motion of a DP vessel is relatively low-frequency motion, the cut-off frequency should be small. But if the bandwidth is not sufficiently large, it may be not valid for the approximation from a real plant into the nominal model. The cut-off frequency is determined to prevent the linear-wave motion from entering the disturbance observer. The form of the second order Butterworth filter used is as follows:

$$Q(s) = \begin{bmatrix} q(s) & 0 & 0 \\ 0 & q(s) & 0 \\ 0 & 0 & q(s) \end{bmatrix} \tag{41}$$

$$q(s) = \frac{\omega_f^2}{s^2 + 2\zeta\omega_f s + \omega_f^2}$$

Because the disturbance observer makes a real plant into a nominal model without disturbance, it can be known that the performance of the controller is more robust, than the case of using only the controller.

WEATHER-VANING ALGORITHM

To implement the weather-vaning, the disturbance direction has to be defined. The effect of three kinds of disturbances (ocean current, wind and second order wave) is combined, and considered as a single disturbance. When the heading angle (or the opposite heading angle) of a DP vessel is matched with the direction of this single disturbance, the vessel can maintain its position with minimal control force. One can easily find out which quadrant the disturbance direction belongs to in the body-fixed frame. The relations of the disturbance direction and command heading angle ψ_d are listed in Table 1.

Table 1 The disturbance direction estimated by using the sign of the single disturbance.

	The sign of the disturbance		The disturbance direction	Desired heading angle
	Surge force	Sway force		
Case 1	$d_x > 0$	$d_y > 0$	First quadrant	$\psi_d > 0$
Case 2	$d_x > 0$	$d_y < 0$	Second quadrant	$\psi_d < 0$
Case 3	$d_x < 0$	$d_y < 0$	Third quadrant	$\psi_d > 0$
Case 4	$d_x < 0$	$d_y > 0$	Fourth quadrant	$\psi_d < 0$

Case 1 defined in Table 1 is illustrated in Fig. 3.

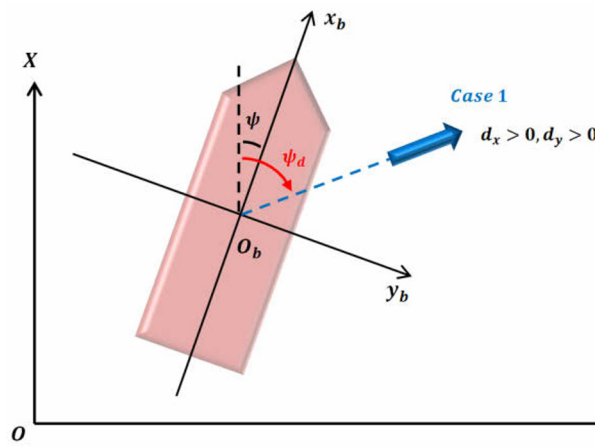


Fig. 3 The relation of the disturbance and the desired heading angle.

If the estimated disturbances in surge and sway axes are all positive, it can be known that the yaw angle, which minimizes the estimated disturbance in the sway axis, exists in the first quadrant in the body-fixed frame. In this case, the desired heading angle is also positive. While the desired heading angle increases, the yaw motion stops at the moment in which the estimated disturbance in the sway axis is small enough. This paper defines the criteria as $d_y^* = 10^2 N$. The rate of the desired heading angle is defined as follows:

$$\dot{\psi}_d(t) = \begin{cases} c \times |\hat{d}_y| - d_y^* & (|\hat{d}_y| > d_y^*, \hat{d}_x \times \hat{d}_y > 0) \\ 0 & (|\hat{d}_y| \leq d_y^*) \\ c \times |\hat{d}_y| + d_y^* & (|\hat{d}_y| > d_y^*, \hat{d}_x \times \hat{d}_y < 0) \end{cases} \quad (42)$$

By the above relation, the desired heading angle is changed. The rate of the desired heading angle is proportional to $|\hat{d}_y|$. This means that if the difference between the vessel's heading angle and the desired heading angle is large, the desired heading angle changes rapidly; if not, it changes slowly. The constant c is 10^{-6} , which is determined by trial and error.

NUMERICAL SIMULATION

The whole flow of the numerical simulation is illustrated in Fig. 4. First of all, the wave-frequency motion is generated by using the ITTC sea spectrum and the motion RAO. The disturbances are composed of the ocean current, wind and wave drift force. The output of the nonlinear DP model enters the feedback loop and the disturbance observer. The estimated disturbance

is the input of the weather-vaning algorithm to calculate the disturbance direction in real-time. The calculated disturbance direction becomes a 3 DOF horizontal reference, input with the desired position. The control input consists of the output of the controller part and the disturbance compensation part.

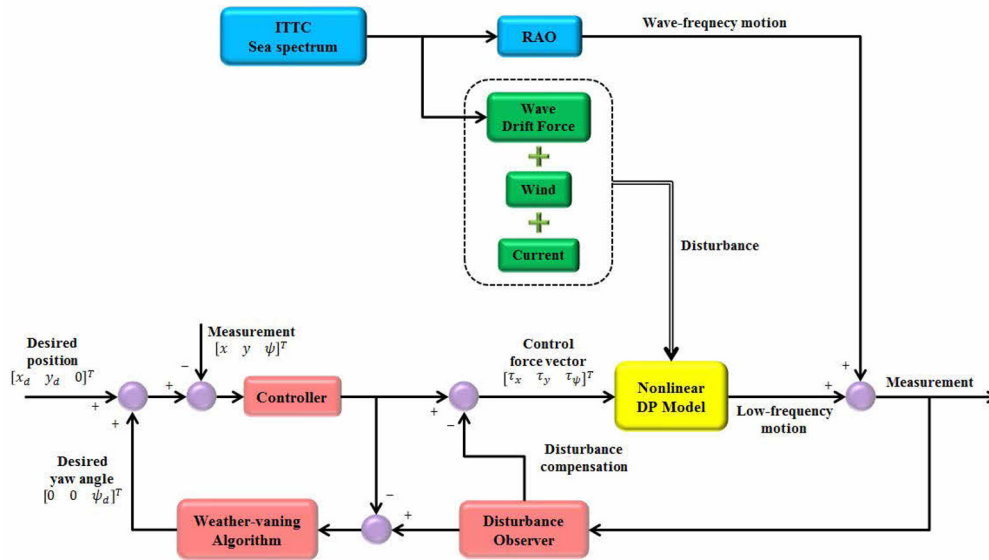


Fig. 4 Whole flow of the simulation for the auto weather-vaning DP control system.

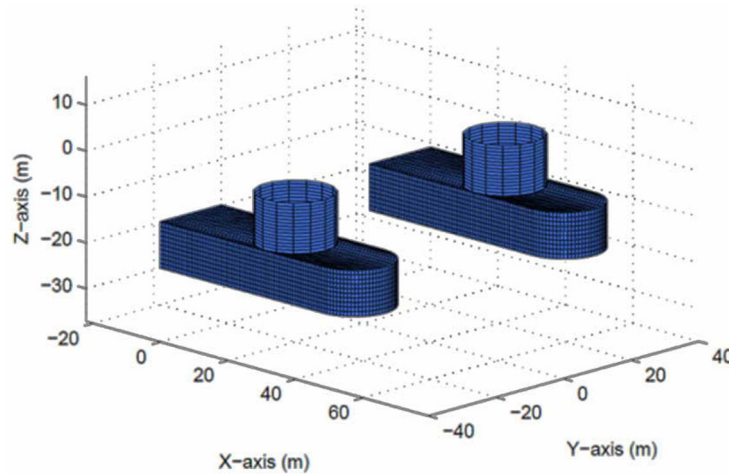


Fig. 5 The front side under structure shape of the semi-submersible type vessel.

The DP vessel used for the numerical simulation is a semi-submersible type vessel. The under structure shape of the vessel is illustrated in Fig. 5. Because the shape is of front-back symmetry, only the front side shape is shown. The main dimensions are listed in Table 2.

Table 2 Main dimensions of the semi-submersible type vessel.

Parameter	Value
M (Mass)	51.980 (tons)
L (Length)	115.0 (m)
B (Breadth)	80.0 (m)
T (Draft)	21.0 (m)

Marine Systems Simulator (MSS) Hydro is used to get the hydrodynamic forces (Perez et al., 2006). The wind load can be calculated from the specific upper structure information of the vessel. This paper assumes the wind load of the semi-submersible vessel is similar to that of a general ship. The wind and wave loads used are illustrated in Figs. 6 and 7.

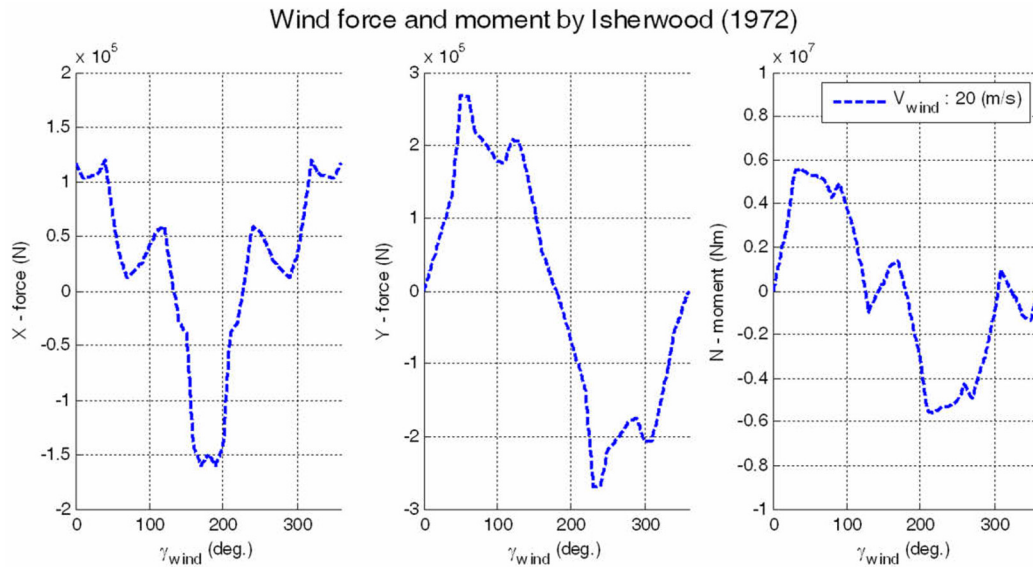


Fig. 6 Wind force and moment with relative heading angle γ_{wind} between the vessel and the wind.

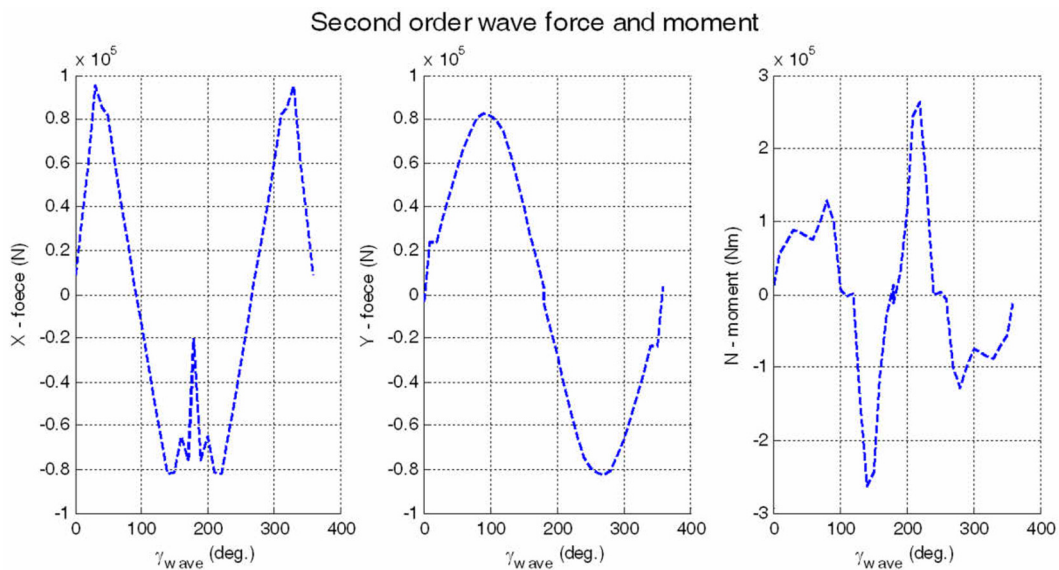


Fig. 7 Second order wave force and moment with relative heading angle γ_{wave} between the vessel and the wave.

The disturbance condition is listed in Table 3. The wind speed and direction, the significant wave height and mean direction, and the ocean current speed and direction are presented. In Fig. 8, ITTC wave spectrum is illustrated. The spectrum is short-crested wave spectrum which has one modal point. In real world, the spectrum may have two or more modal points, so it can not reflect the actual wave condition. But, the focus of this paper is disturbance rejection and weather-vaning. The number of modal points does not affect the performance of proposed controller and disturbance observer because the cut-off frequency of the disturbance observer has to be determined by the frequency bandwidth of ocean disturbances. Thus, it does not matter which shape of spectrum is used. In order to check the performance with the most extreme conditions, all disturbance directions are 90° .

Table 3 Disturbance conditions.

Disturbance		Value
Wind	Speed	20(knot)
	Dir.	90(deg.)
Wave	H _{1/3} (Significant wave height)	3(m)
	Modal Period	9.5157(sec.)
	Mean Dir.	90(deg.)
Ocean current	Speed	0.2(m/s)
	Dir.	90(deg.)

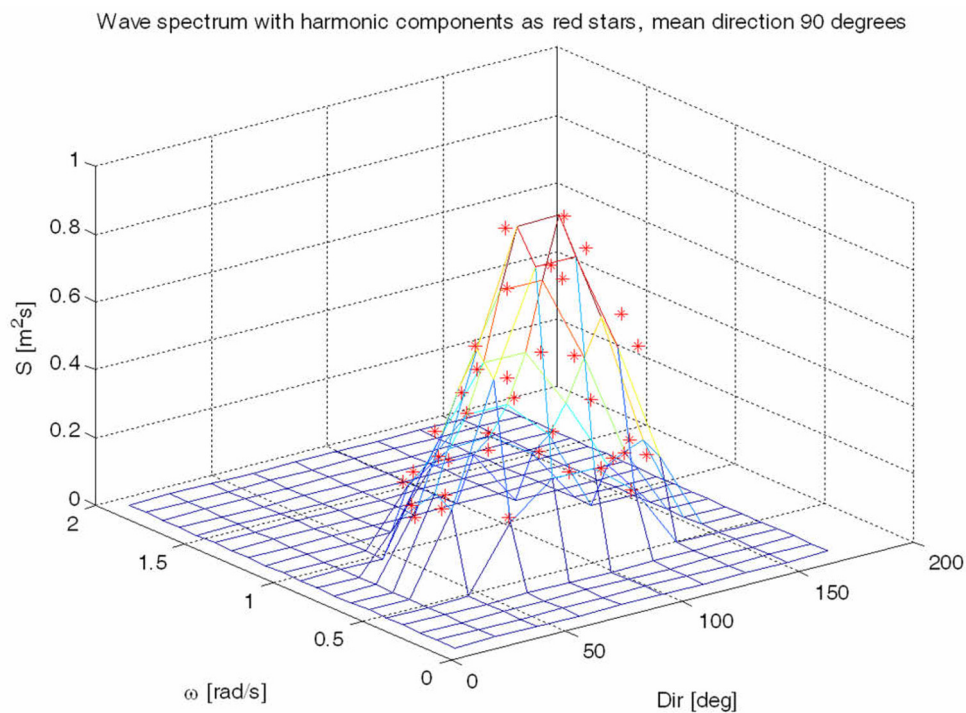


Fig. 8 ITTC wave spectrum (modal period = 9.5157(sec.), significant wave height = 3m).

Actually, the control force vector has to be allocated actuators like propellers or thrusters, which are installed on the DP vessel. This is another problem, which is called the control allocation. In particular, most semi-submersible type vessels have azimuth thrusters that have two degree movement freedom (azimuth angle, and thrust). This is a nonlinear control allocation problem, which is not covered in this paper. Instead, in order to consider indirectly the effect of actuators, first order systems are used, as follows:

$$\begin{aligned}
 T_x \dot{\tau}_x + \tau_x &= \tau_{x,com} \\
 T_y \dot{\tau}_y + \tau_y &= \tau_{y,com} \\
 T_\psi \dot{\tau}_\psi + \tau_\psi &= \tau_{\psi,com}
 \end{aligned}
 \tag{43}$$

where, $\tau_{x,com}$, $\tau_{y,com}$ and $\tau_{\psi,com}$ are the command control force and moment. $[T_x \ T_y \ T_\psi]$ is the time constant $[5 \ 5 \ 5]$. The unit is seconds. The cut-off frequency of the disturbance observer and the low-pass filter is 0.1seconds in reference [Fossen](#)

(2002). The controller gain matrices K_1 and K_2 are as follows:

$$K_1 = \begin{bmatrix} 0.05 & 0 & 0 \\ 0 & 0.05 & 0 \\ 0 & 0 & 0.05 \end{bmatrix}, K_2 = \begin{bmatrix} 0.1 & 0 & 0 \\ 0 & 0.1 & 0 \\ 0 & 0 & 0.5 \end{bmatrix} \quad (44)$$

The time responses of the position vector and the control force vector are shown in Figs. 7 and 8. The simulation time is 600 seconds. To show robustness of disturbance observer based controller, simulations are performed about the case using only controller and the other case using not controller but disturbance observer. The simulation results are in Fig. 9. In the case of no disturbance rejection by disturbance observer, there is steady state error compared with the case with disturbance rejection, although the control gain matrix is the same.

Comparison of position vector with and without the disturbance observer ($\psi_{wind} = \psi_{wave} = \psi_{current} = 90^\circ$)

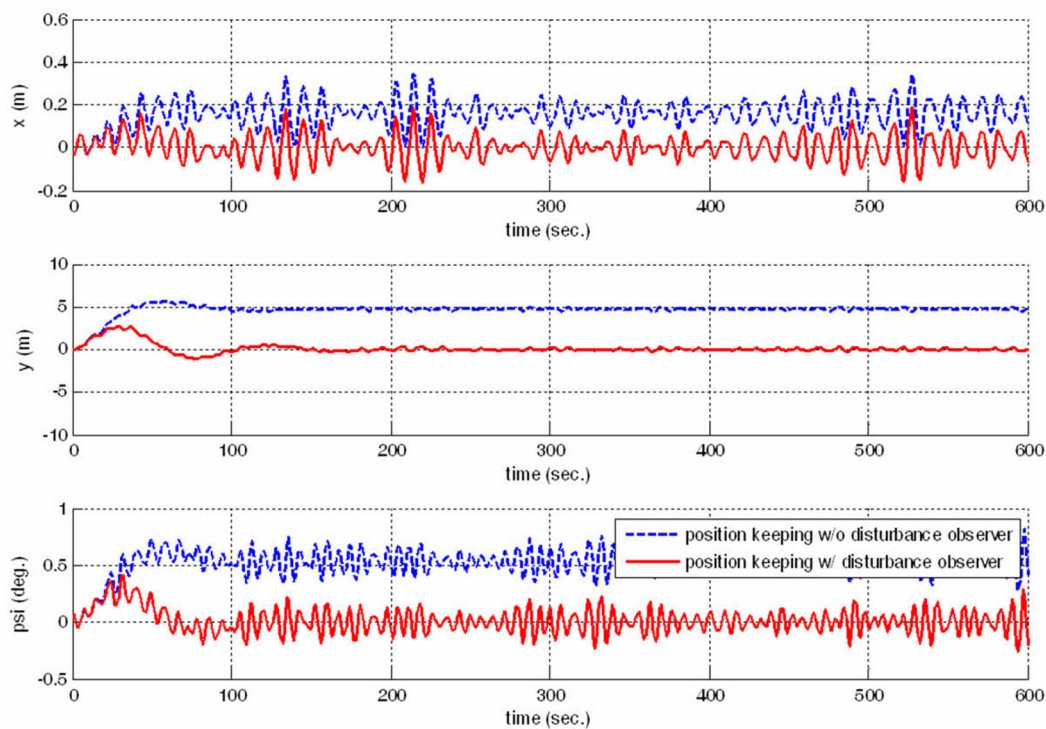


Fig. 9 Comparison of position vector with and without the disturbance observer.

The other simulation is about comparison according to the presence of weather-vaning. The simulation results in Figs. 10 and 11. In Fig. 10, it seems that the case of not using weather-vaning is more efficient for position keeping than the case of using weather-vaning. But the position error is less than 1m, so it can be said that the error is trivial. By the weather-vaning algorithm, the vessel's heading angle changes continuously, and eventually heads for the disturbance direction of 90°. Through Fig. 12, proposed disturbance observer well reject real disturbance. In the steady state, it can be considered the estimated disturbance is approximated real disturbance. Without the weather-vaning, the relative angle between the vessel and the disturbance is 90°, so the surge control force is almost zero and the sway control force exists somehow. In contrast to this, with the weather-vaning, the relative angle between the vessel and the disturbance goes to 0°, so the surge control force exists somehow, and the sway control force is almost zero. To compare the surge and sway the control forces, the norm value of control forces is calculated.

Comparison of position vector with and without weather-vaning ($\psi_{wind} = \psi_{wave} = \psi_{current} = 90^\circ$)

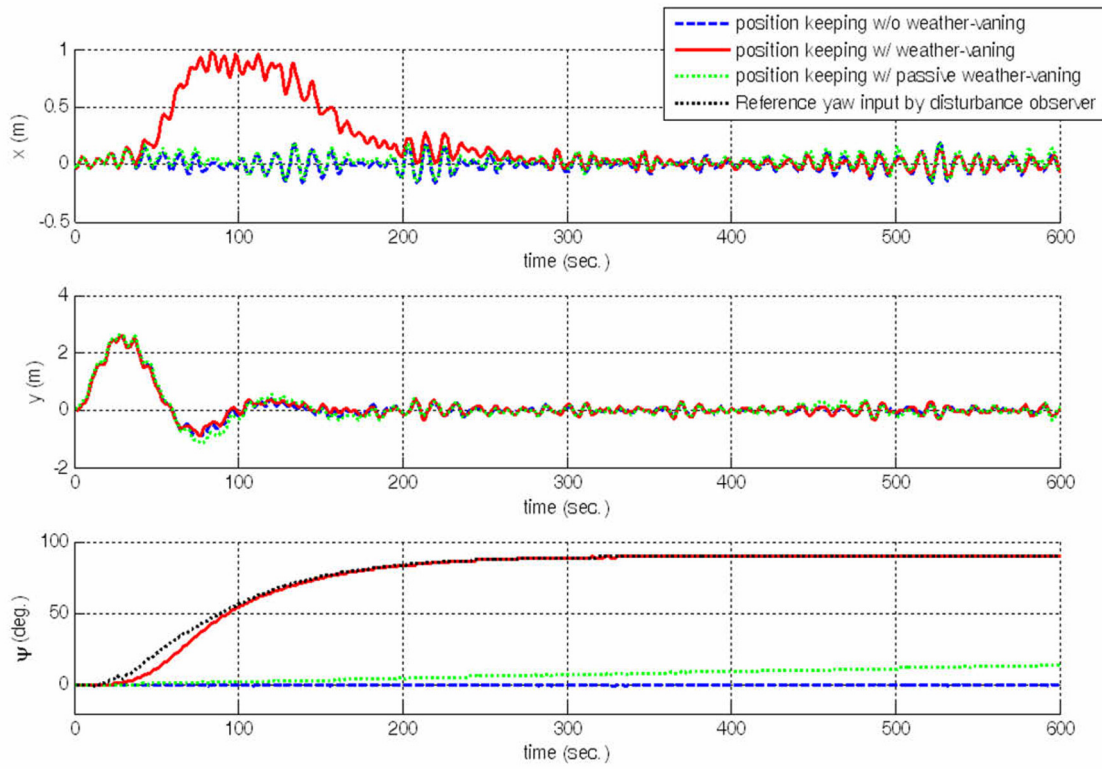


Fig. 10 Comparison of position vector with and without weather-vaning.

Comparison of control force vector with and without weather-vaning ($\psi_{wind} = \psi_{wave} = \psi_{current} = 90^\circ$)

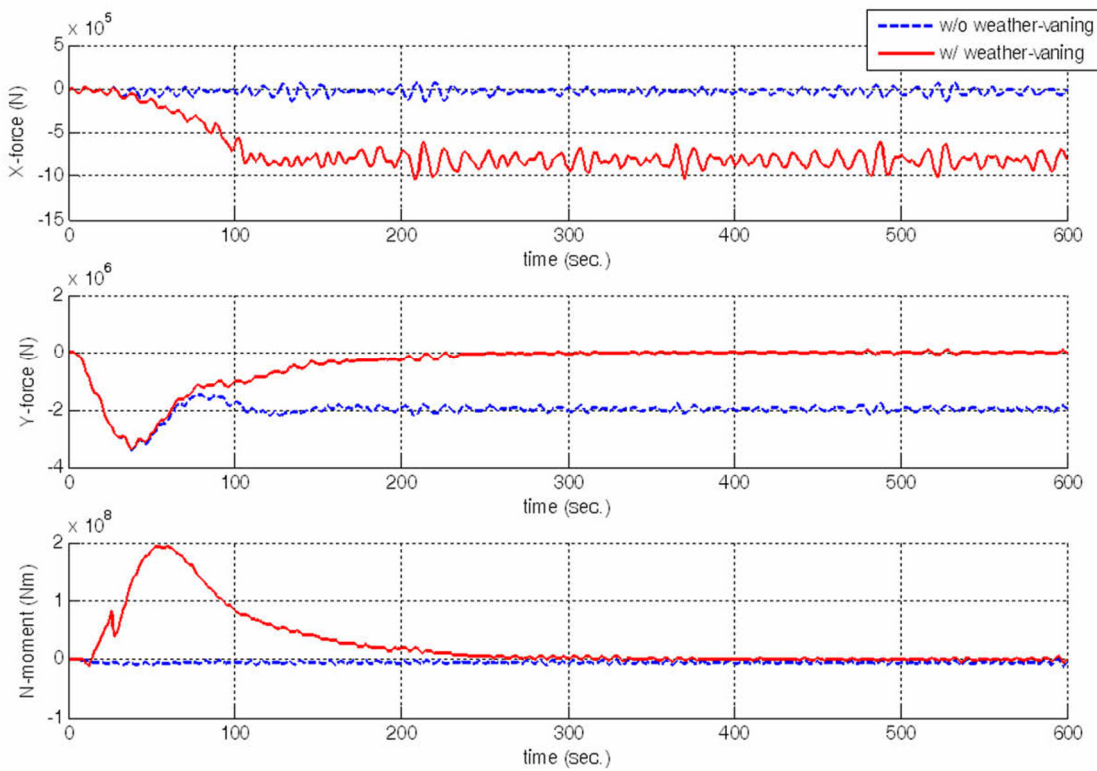


Fig. 11 Comparison of control force vector with and without weather-vaning.

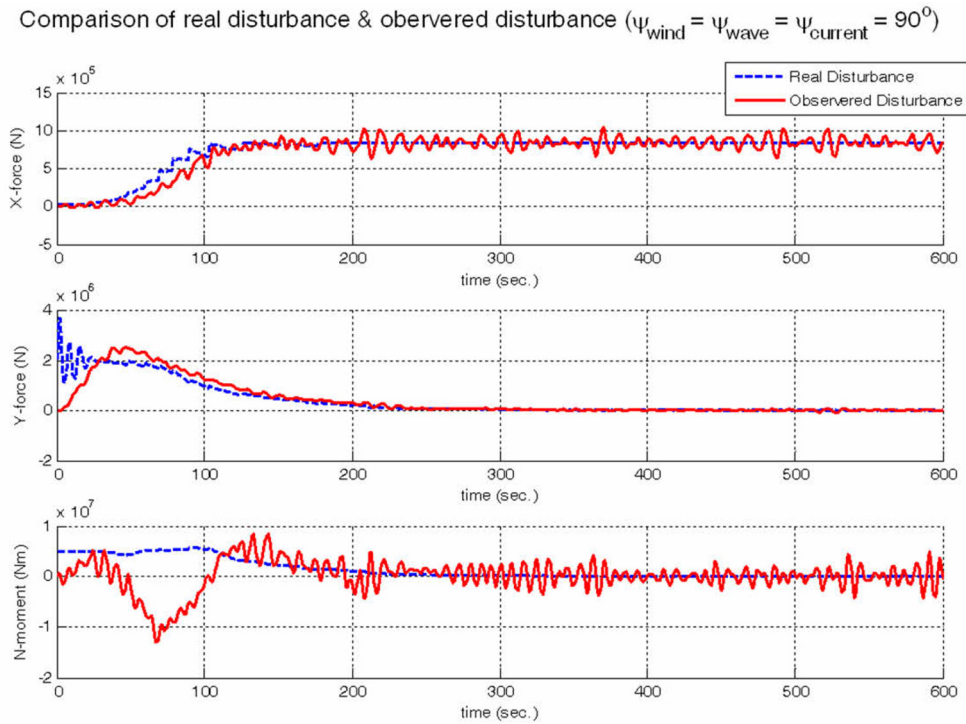


Fig. 12 Comparison of the real disturbance and the observed disturbance.

After about 80s, the sway control force becomes smaller than the surge control force and after about 200s, the mean values of the two control forces are not changed. This means that the vessel heads for the disturbance direction after about 200s.

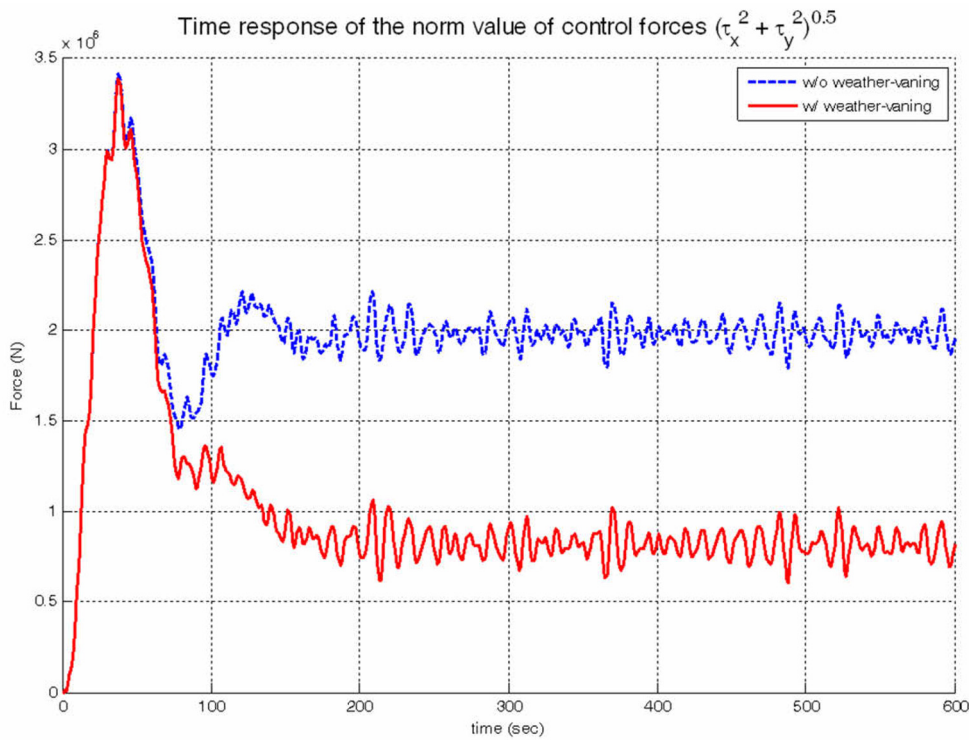


Fig. 13 Time response of the norm value of control forces.

To verify proposed method in various direction of disturbances sea conditions, simulations are performed in the combination of the four kinds of disturbance directions.

Table 4 Disturbance conditions.

Direction	Wave	Wind	Current
Condition 1	30°	45°	60°
Condition 2	30°	45°	90°
Condition 3	30°	60°	90°
Condition 4	45°	60°	90°

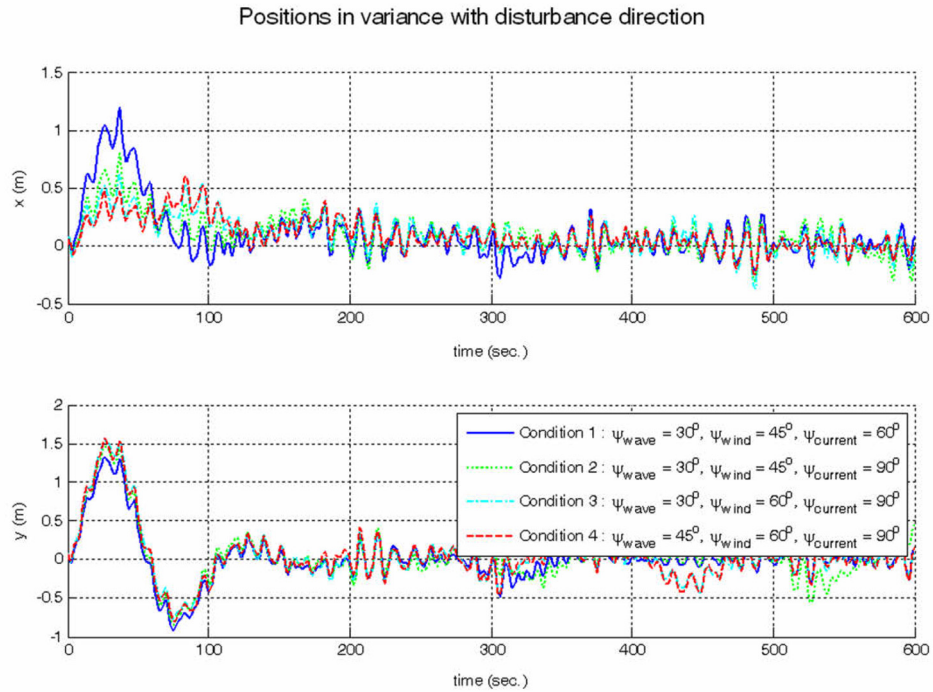


Fig. 14 Positions in variance with disturbance directions.

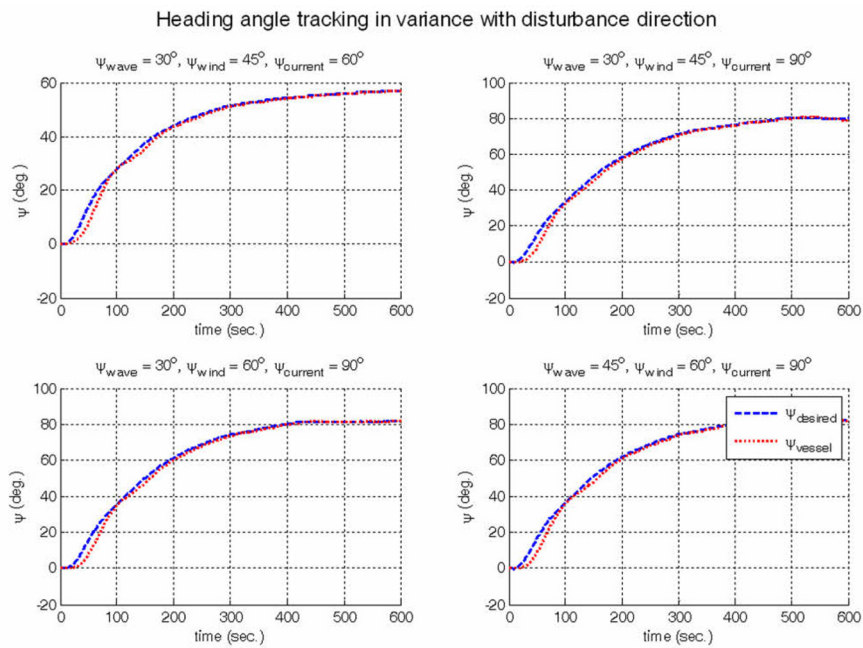


Fig. 15 Heading angle tracking in variance with disturbance directions.

In Fig. 14 and in Fig. 15, although the directions of disturbance are not the same and different each other, it is shown that the position keeping and the heading angle tracking are well performed.

To check whether the weather-vaning algorithm enables the control forces to minimize or not, the integration of control force with heading angle of the DP vessel from 0° to 180° with interval degrees 10° is performed.

$$F_{total} = \int_0^T \sqrt{\tau_x^2 + \tau_y^2} dt, \quad T = 600(sec) \tag{45}$$

The comparison results is in Fig. 14.

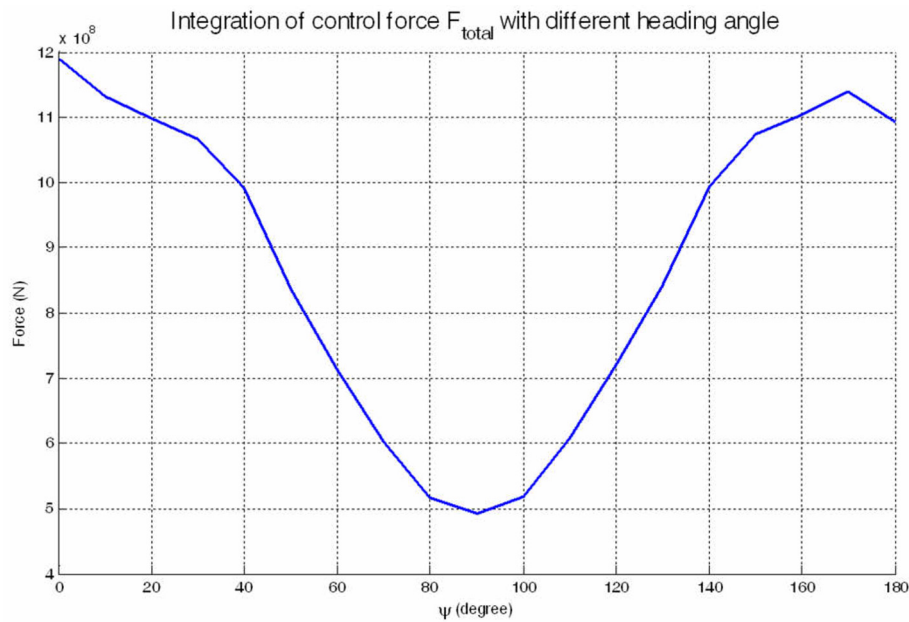


Fig. 16 The integration of control force F_{total} with the disturbance observer.

In Fig. 14, the minimum point appears at about a heading angle 90°. This is a reasonable result in the consideration of the disturbance conditions of Table 3. By this, the proposed weather-vaning system enables the DP vessel to keep its position, with the minimum control force. Thus it can be known that the ocean operations are performed in not only a stable but also an economically efficient condition.

CONCLUSIONS

The paper presents an auto weather-vaning system for a DP vessel. The mathematical model of a DP vessel is constructed. The model is divided into two parts, the wave-frequency model and the low-frequency model. The kinds of disturbances (ocean current, wave and wind) are described. The disturbance observer is designed to eliminate the effect of ocean disturbances, and to estimate the disturbance direction. The backstepping controller is designed to not only maintain the position, but also to implement the weather-vaning algorithm. The weather-vaning algorithm can determine the disturbance direction by using the estimated disturbance, which is the output of the disturbance observer in real time. Finally, two numerical simulations are performed for a semi-submersible type vessel. The one is about disturbance rejection performance by comparison of the presence of disturbance observer. The other is about weather-vaning performance by comparison of the presence of weather-vaning algorithm. The results show that the proposed method make a DP vessel maintain its position with the minimum control force.

ACKNOWLEDGMENT

This research was supported by Basic Science Research Program through the National Research Foundation of Korea (NRF) funded by the Ministry of Education, Science and Technology (NRF-2012R1A1A2008683).

REFERENCES

- Blendermann, W., 1995. Estimation of wind loads on ships in wind with a strong gradient. *Proceedings of the 14th International Conference on Offshore Mechanics and Arctic Engineering (OMAE)*, Copenhagen, Denmark, 18-22 June 1995, v1-A, pp.271-277.
- Chillamcharla, G.K., Thiagarajan, K.P. and Winsor, F., 2009. Mooring analysis of a weathervaning FPSO in bi-directional sea-states. *Proceedings of ASME 2009 28th International Conference on Ocean, Offshore and Arctic Engineering*, 6, pp.585-590.
- Choi, Y., Yang, K., Chung, W.K., Kim, H.R. and Suh, I.H., 2003. On the robustness and performance of disturbance observers for second order systems. *IEEE Transactions on Automatic Control*, 48(2), pp.315-320.
- Faltinsen, O.M., 1990. *Sea loads on ships and offshore structures*. Cambridge: Cambridge University Press.
- Fossen, T.I., 1994. *Guidance and control of ocean vehicles*. New York: John Wiley and Sons.
- Fossen, T.I. and Strand, J.P., 2001. Nonlinear passive weather optimal positioning control (WOPC) system for ships and rigs: Experimental results. *Automatica*, 37(5), pp.701-715.
- Fossen, T.I., 2002. *Marine control systems: guidance, navigation and control of ships, rigs and underwater vehicles*. Trondheim: Marine Cybernetics.
- Gould, R.W.F., 1982. The estimation of wind loads on ship superstructures. *The Royal Institution of Naval Architects, monograph*, 8, p.34.
- Isherwood, R.M., 1972. Wind resistance of merchant ships. *Transportation Royal Institution of Naval Architects*, 1972 (114), pp.327-338.
- Khalil, H.K., 2002. *Nonlinear systems*. 3rd ed. New Jersey: Prentice-Hall.
- Kitamura, F., Sato, H., Shimada, K. and Mikami, T., 1997. Estimation of wind force acting on huge floating ocean structures. *Proceedings of the Oceans '97. MTS/IEEE Conference*, Canada, Halifax, 6-9 October 1997, 1, pp.197-202.
- Kokotovic, P.V., 1992. The joy of feedback: nonlinear and adaptive. *Control Systems Magazine, IEEE*, 12(3), pp.7-17.
- Lee, C.H., Kim, T.H. and Tahk, M.J. 2011. Missile autopilot design for agile turn using time delay control with nonlinear observer. *International Journal of Aeronautical & Space Sciences*, 12(3), pp.266-273.
- Lewis, E.V.Ed., 1989. *Principles of naval architecture*. 2nd ed. New Jersey: Society of Naval Architects and Marine Engineers (SNAME).
- Lozano, R. and Brogliato, B., 1992. Adaptive control of robot manipulators with flexible joints. *IEEE Transactions on Automatic Control*, 37(2), pp.174-181.
- Morandini, C. and Wong, J., 2007. Heading analysis of weathervaning floating structures: why, how and where to make the best of them. *Proceedings of the Seventeenth International Offshore and Polar Engineering Conference*, Lisbon, Portugal, 1-6 July 2007, pp.276-283.
- Newman, J.N., 1977. *Marine hydrodynamics*. Cambridge: MIT Press.
- OCIMF, 1994. *Prediction of wind loads and current loads on VLCCs*. London: Witherby.
- Perez, T., Smogeli, Ø.N., Fossen, T.I. and Sørensen, A.J., 2006. An overview of the marine systems simulator (MSS): A simulink toolbox for marine control systems. *Modeling, identification and Control*, 27(4), pp.259-275.
- Radke, A. and Gao, Z., 2006. A survey of state and disturbance observers for practitioners. *Proceedings of Conference Decision and Control*, Minneapolis, MN, 14-16 June 2006, pp.5183-5188.
- Schrijver, E. and van Dijk, J., 2002. Disturbance observers for rigid mechanical systems: equivalence, stability, and design. *Journal of Dynamic Systems, Measurement, and Control*, 124(1), pp.539-548.
- Shim, H.B. and Joo, Y., 2007. State space analysis of disturbance observer and a robust stability condition. *Proceedings of Conference Decision and Control*, New Orleans, LA, USA. 12-14 December 2007, pp.2193-2198.
- Shim, H.B. and Jo, N.H., 2009. An almost necessary and sufficient condition for robust stability of closed-loop systems with disturbance observer. *Automatica*, 45(1), pp.297-299.
- Sørensen, A.J., 1996. Design of a dynamic positioning system using model based control. *Journal of Control Engineering Practice*, 4(3), pp.359-368.
- Sørensen, A.J., 2011. A survey of dynamic positioning control systems. *Annual Reviews in Control*, 35(1), pp.123-136.